Received: 29 April 2020 | Revised: 22 January 2021 | Accepted: 13 March 2021

DOI: 10.1111/nan.12714

Neuropathology and Applied Neurobiology WILEY

ORIGINAL ARTICLE

TGF-β activates pericytes via induction of the epithelial-to-mesenchymal transition protein SLUG in glioblastoma

Naita M. Wirsik[1,2] | Jakob Ehlers[3,4] | Lisa Mäder[1,5] | Elena I. Ilina[1,6,7] | Anna-Eva Blank[1,8] | Anne Grote[9] | Friedrich Feuerhake[9,10] | Peter Baumgarten[1,11] | Kavi Devraj[1,12] | Patrick N. Harter[1,12,13,14] | Michel Mittelbronn[1,6,7,15,16] | Ulrike Naumann[3]

[1]Edinger Institute (Neurological Institute), Goethe University Hospital, Frankfurt/Main, Germany

[2]General-, Visceral- and Transplantation Surgery, University Hospital Heidelberg, Heidelberg, Germany

[3]Laboratory of Molecular Neuro-Oncology, Department of Vascular Neurology, Hertie Institute for Clinical Brain Research, University of Tübingen, Tübingen, Germany

[4]Department of Radiation Oncology, University Hospital Tübingen, Tübingen, Germany

[5]Department of Neurology, Klinikum Darmstadt, Darmstadt, Germany

[6]Luxembourg Centre of Neuropathology (LCNP), Luxembourg, Luxembourg

[7]Department of Oncology (DONC), Luxembourg Institute of Health (LIH), Luxembourg, Luxembourg

[8]Pediatric Cardiology, University Hospital of Giessen, Gießen, Germany

[9]Institute for Pathology, Hannover Medical School, Hannover, Germany

[10]Institute for Neuropathology, University Clinic Freiburg, Freiburg, Germany

[11]Department of Neurosurgery, Goethe University, Frankfurt/Main, Germany

[12]German Cancer Consortium (DKTK), Heidelberg, Germany

[13]German Cancer Research Center (DKFZ), Heidelberg, Germany

[14]Frankfurt Cancer Institute (FCI), Frankfurt am Main, Germany

[15]Luxembourg Centre for Systems Biomedicine (LCSB), University of Luxembourg, Luxembourg, Luxembourg

[16]National Center of Pathology (NCP), Laboratoire Nationale de Santé (LNS), Luxembourg, Luxembourg

Correspondence
Prof. Dr Michel Mittelbronn, Department of Oncology (DONC), Luxembourg Center of Neuropathology (LCNP), Luxembourg Institute of Health (LIH), 84, Val Fleuri, L-1526 Luxembourg, Luxembourg.
Email: michel.mittelbronn@lih.lu

Abstract

Aims: In primary central nervous system tumours, epithelial-to-mesenchymal transition (EMT) gene expression is associated with increased malignancy. However, it has also been shown that EMT factors in gliomas are almost exclusively expressed by glioma vessel-associated pericytes (GA-Peris). In this study, we aimed to identify the mechanism of EMT in GA-Peris and its impact on angiogenic processes.

Methods: In glioma patients, vascular density and the expression of the pericytic markers platelet derived growth factor receptor (PDGFR)-β and smooth muscle actin (αSMA) were examined in relation to the expression of the EMT transcription factor SLUG and were correlated with survival of patients with glioblastoma (GBM). Functional mechanisms of SLUG regulation and the effects on primary human brain vascular pericytes (HBVP) were studied in vitro by measuring proliferation, cell motility and growth characteristics.

Michel Mittelbronn and Ulrike Naumann contribute equally for authorship.

Results: The number of PDGFR-β- and αSMA-positive pericytes did not change with increased malignancy nor showed an association with the survival of GBM patients. However, SLUG-expressing pericytes displayed considerable morphological changes in GBM-associated vessels, and TGF-β induced SLUG upregulation led to enhanced proliferation, motility and altered growth patterns in HBVP. Downregulation of SLUG or addition of a TGF-β antagonising antibody abolished these effects.

Conclusions: We provide evidence that in GA-Peris, elevated SLUG expression is mediated by TGF-β, a cytokine secreted by most glioma cells, indicating that the latter actively modulate neovascularisation not only by modulating endothelial cells, but also by influencing pericytes. This process might be responsible for the formation of an unstructured tumour vasculature as well as for the breakdown of the blood–brain barrier in GBM.

KEYWORDS
pericytes, EMT, SLUG, TGF-β

INTRODUCTION

High-grade primary central nervous system tumours, especially glioblastoma (GBM), are the most common brain tumours in adults. The prognosis of GBM is very poor, and even best standard care and therapy raise the median survival by only a few months. Today, no therapy is available to cure these tumours.[1] Common features of GBM are, besides their proliferation and drug resistance, tumour-mediated immunosuppression, the potential to actively invade the healthy brain, and their highly angiogenic properties. GBM-associated angiogenesis is mainly mediated by hypoxia and/or glioma-secreted TGF-β.[2–4]

During development, the epithelial-to-mesenchymal transition (EMT) plays a crucial role in body patterning and the differentiation of multiple tissues. In contrast, reactivation of EMT genes in adult tissues is associated with tumour initiation and progression, tumour cell invasion and metastasis.[5–10] Previous analysis of different mRNA signatures of GBM led to the proposition of a new stratification of GBM subgroups, in which the mesenchymal mRNA signature profile has been associated with more frequent recurrences and higher malignancy.[11] More recent studies showed that the rather more benign pilocytic astrocytoma (World Health Organization, WHO grade I) also displayed a mesenchymal signature,[12] which at least partly contradicts the hypothesis that, in glioma, the mesenchymal signature is associated with increased malignancy.[13] A possible reason for the correlation of the mesenchymal signature with a poor prognosis might be that the EMT factor expression in glioma was analysed at the mRNA level [14] instead of determining protein levels and identifying the cell type that expresses specific EMT proteins. Additionally, knowing that the EMT programme is induced by TGF-β in cancer [15,16] and knowing that high-grade gliomas (HGG) secrete high levels of TGF-β,[17] this might explain why the mesenchymal signature in glioma is connected to its poor prognosis.

Recently, we have identified EMT transcriptional regulator proteins like SLUG, encoded by the SNAI2 gene, or TWIST, to be almost exclusively expressed in pericytes of glioma vascular proliferations, but neither in 'normal' pericytes covering vessels in the adjacent healthy brain, nor in endothelial or glioma cells.[12] Pericytes are important regulators of the vessel structure in the brain and indispensable to maintain blood–brain barrier (BBB) integrity (for review see [18]). Numerous markers have been proposed to characterise pericytes in vivo and in vitro, such as platelet derived growth factor receptor (PDGFR)-β, neuron-glial antigen 2 (NG2), CD146, or smooth muscle actin (αSMA). While NG2 and CD146 seemed to be ubiquitous pericytic markers, PDGFR-β was found especially on capillary-associated pericytes.[12] In GBM, it has been shown that glioma cells are able to change pericytes from a tumour-suppressive towards an immature and immune-suppressive cell type, thereby triggering tumour progression.[19,20] However, little is known about the underlying mechanisms of how GBM pericytes become activated and start to divide within the vascular proliferations. Additionally, little is known about the signalling pathways that glioma cells use to (a) modulate the function of pericytes during tumour vascularisation and (b) modify capillary structures and BBB integrity. In the present study, we investigate the effects of an EMT program activation in human brain microvascular pericytes (HBVP) with a focus on TGF-β and the EMT transcription factor SLUG.

MATERIAL AND METHODS

Cells, viruses and reagents

LN-229 and LN-308 human glioma cells were kindly provided by M. Hegi (Lausanne, Switzerland). The cells have been described in detail in.[21] Glioma cells were maintained in Dulbecco's modified Eagle's medium (DMEM; Sigma-Aldrich) containing 10% fetal calf serum (FCS; GIBCO Life Technologies), penicillin (100 U/ml) and streptomycin (100 μg/ml). Primary HBVPs were purchased by ScienCell. HBVPs were maintained in pericyte basal medium

supplemented with 2% inactivated FCS, 1% of pericyte growth supplement (PGS), penicillin (100 U/ml), streptomycin (100 µg/ml, all ScienCell) in flasks coated with poly-L-lysine (Sigma-Aldrich). The cell lines were routinely tested to be free of Mycoplasma using the MycoAlert™ Mycoplasma Detection Kit (Lonza GmbH). To generate conditioned medium, GBM cells were cultivated in pericyte basal medium for 24 h. Supernatants (SN) were collected and clarified of cellular debris by centrifugation. After addition of 1% PGS, SN were used to culture HBVP. To treat HBVP with recombinant human TGF-β1 and/or -β2 (PeproTech GmbH), cells were cultured in FCS depleted pericyte medium. To block TGF-β activity, a pan-TGF-β-neutralising antibody (clone 1D11, # MA5-23795; ThermoFisher Scientific) was added to the TGF-β containing medium in a 100-fold excess. Ad-SLUG and Ad-EGFP were prepared as previously described.[22] Ad-SLUG additionally codes for EGFP in a second expression cassette. Infection with recombinant adenoviruses was accomplished by exposing HBVP to 30 MOI of the appropriate adenovirus in serum-deprived pericyte medium for 15 min, followed by the addition of supplemented medium as described above.

si-RNA transfection

To transiently knockdown SLUG in HBVPs, a pool of 30 human SLUG-specific siRNAs (siTOOL) was used. As a negative control, a pool of 30 unspecific, non-target siRNAs (SF) was used. siRNAs were transfected using Lipofectamine 2000 (ThermoFisher Scientific) according to the provider´s protocol. Analyses were performed 72 h after transfection.

RT-PCR

For reverse transcription polymerase chain reaction (RT-PCR), RNA of treated and untreated cells was isolated using the RNApure isolation kit (Machery and Nagel) and transcribed into cDNA using M-MuLV reverse transcriptase (New England Biolabs). Quantitative PCR was performed using the ORA qPCR Mix (HighQu) on a Roche Light Cycler 96 (Roche). Cycling conditions were as following: 95°C for 3 min, 45 cycles at 95°C for 10 s and 60°C for 30 s. The following primers were designed based of the gene´s cDNA sequence: αSMA (NM001613): forward 5′-GGCACCCCTGAACCCCAAGG-3′; reverse 5′-GCACGATGCCAG TTGTGCGT-3′. SLUG (NM003068): forward 5′-GCGAACTGGACAC ACATACAGTGAT-3′; reverse 5′-GGAGCAGCGGTAGTCCACACA-3′. β-Actin (NM_001101): forward 5′-GCACTCTTCCAGCCTTCCTT-3′; reverse 5′-GTTGGCGTACAGGTCTTTGC-3′′. For standard RT-PCR, the following primers and Taq-polymerase from Sigma-Aldrich were used: GAPDH forward 5′-TGCACCACCAACTGCTTAGC-3′; GAPDH reverse 5′-GGCATGGAC TGTGGTCATGAG-3′; αSMA forward 5′-CAGCTTCCCTGAACACCACC-3′; αSMA reverse 5′-ACGCTCAGCAGT AGTAACGA-3′; SLUG forward 5′-ACGCCCAGCTA CCCAATGGC-3′; SLUG reverse 5′-AGGCTTCTCCCCCGTGTGAGTT-3′.

Immunoblot analysis

The general immunoblot procedure has been described elsewhere.[23] Protein contents were analysed according to Bradford. Following antibodies were used: tubulin (sc-12462-R; Santa Cruz Biotechnology), αSMA (CBL171; Merck/Millipore), SLUG (clone C19G7, # 9585; Cell Signaling), pSMAD2$^{S465/467}$ (clone 138D4, #3108S; Cell Signaling), SMAD2/3 (#3102; Cell Signaling), TGF-β-R2 (clone H-567, sc-1700; Santa Cruz Biotechnology). Blots were analysed and quantified using the WesternBright Chemiluminescence detection kit (Biozym) on a Lumi-Imager and the appropriate quantification software ImageLab (both Biorad Laboratories GmbH).

Patient tissue and tissue microarrays (TMA)

In total, 351 tissue samples from patients with brain tumours were investigated comprising 47 pilocytic astrocytomas (WHO I), 16 astrocytomas (WHO II), 35 astrocytomas (WHO III) and 253 GBM (WHO IV). Fifty-four normal brain tissue samples from autopsy cases, histologically normal-appearing brain tissue surrounding GBM samples and human tonsil tissue were used as controls. The samples were obtained from the tissue bank of the Edinger Institute (Neurological Institute), Frankfurt, Germany. Tissue samples were fixed in 4% buffered formalin (Roth) and embedded in paraffin. Tissue microarrays (TMAs) were constructed by punching 896 representative tissue cores from paraffin blocks of the before mentioned cohort (e.g. infiltration zone, tumour centre, normal-appearing brain tissue), reintegrating them into preformed holes of recipient paraffin blocks. The histopathological diagnoses were performed according to the WHO criteria by experienced neuropathologists (MM, PNH). The use of patient material was approved by the local ethics committee (GS-04/09 and GS-249/11).

Scoring

PDGFR and αSMA expression were separately assessed in vessel-associated and tumour cells taking into account the staining intensity (0: no, 1: weak, 2: moderate, 3: strong) and frequency (0: 0%–1%, 1: 1%–10%, 2: 10%–25%, 3: 25%–50% and 4: >50%) of all cells showing positive staining. Both scores were multiplied to determine the final score (see Figure S1).

Microscopy and determination of vessel area using automated image analysis

To determine morphological alteration in HBVP, photographs were taken on a Zeiss Imager Z1 microscope using the Zeiss Axiovision software (Carl Zeiss). TMA slides stained for CD31 (clone JC70A; Dako/Agilent) were scanned with a resolution of 0.253 µm/pixel (40x) using an Aperio AT2 Scanner (Leica Microsystems). The

slides were automatically analysed using a program written in MATLAB (Natick). TMA spots on the scanned slide images were detected automatically in low resolution with following manual correction for some slides. Consecutively, each spot image was analysed in high resolution to detect vessel areas. To determine the area of vessels, colour deconvolution [24] was applied to each spot image to obtain a 3,3′-diaminobenzidin (DAB) image. The DAB image was analysed with an estimated threshold using a minimum cross-entropy method.[25] Detected DAB regions were smoothed using morphological operations (opening and closing) to delete small regions and connect close regions. The number and total area of vessel regions as well as the ratio of vessel count and vessel area (count/area) were determined from the DAB regions for each spot. In order to obtain a meaningful number for the ratio, the vessel area was normalised by the average area of one vessel region, which was determined by computing the average area from all analysed spots. In this way, a ratio value >1 means that areas of single vessel objects are relatively small compared to the average, and a ratio value <1 means that areas of single vessel objects are relatively big.

Growth pattern analyses of HBVP

To determine the growth pattern of HBVP, the cells were seeded on PLL-coated plates, were treated and photographs were taken using an Olympus reflex camera. Star-like clusters were quantified by presenting the percentage of cell in clusters after manually counting total cells and cells that are part of a cluster.

Proliferation and viability assays

The cell proliferation rate was assessed over 5 days. In total, 1000 cells/well were seeded at four technical replicates per condition into 96-well plates. Cell density was determined by crystal violet staining every second day.[26] Additionally, mitochondrial activity was determined 72 h after treatment using the MTT or WST1 assay. For these assays, HBVPs were seeded in 96-well plates at a density of 1×10^5 cells/ml and allowed to attach. Cells were cultured in serum-derived medium as a control, in the presence of TGF-β1 and/or -β2 (10 ng/ml), or in SN prepared from LN-229 glioma cells. After treatment, the medium was removed and mitochondrial activity was determined by the addition of MTT [27] or WST1 assay according to the providers protocols. The optical density (OD_{560}) was determined on an infinite M200 pro plate reader. Analyses were performed in quadruplicates.

Cell migration

The Boyden chamber migration assay has been previously described in detail.[28] Migration was analysed 24 h after treatment, or 72 h after siRNA transfection for a period of 24 h. Analyses consisted of the counting of migrated cells in seven regions of interest (ROIs) per membrane at the Olympus BX1 microscope (Olympus) using a 40x magnification objective. At least two membranes per biological replicate (n = 3) were taken for statistical analyses.

Statistical analyses

The semi-quantitative PDGFR-β and αSMA scores were treated as ordinal variables. Response variables and statistical differences among WHO grades in TMA data were assessed using the non-parametric Wilcoxon test followed by the Bonferroni post hoc test. The ratio vessel count/area (for automated CD31 staining analysis) was analysed using the Tukey's honestly significant difference (HSD) test. Ordinal data were analysed using a contingency table followed by Pearson's chi-squared test. Growth patterns of HVBP cultures were statistically analysed using the Welch's unequal variances two tailed t-test. The association of patient survival with the response variable (PDGFR-β or αSMA expression as well as vessel count/area for CD31 immunohistochemistry) was assessed by Kaplan–Meier analysis tested by the log-rank and Wilcoxon test. Proliferation, migration and metabolic activity changes were analysed using ANOVA followed by Tukey's test. Statistical analyses were performed using JMP 8.0 software (SAS). A significance level of alpha = 0.05 was selected for all tests. Graphs were prepared using Excel (Microsoft) or GraphPad Prism (GraphPad Software Inc.). The gene expression correlation analyses were performed using the 'R2: Genomics Analysis and Visualization Platform (http://r2.amc.nl). On this platform, 540 samples from the TCGA glioblastoma cohort (R2 internal identifier: ps_avgpres_broadgbm540_u133a) were analysed.

RESULTS

SLUG expression strongly correlates with the expression of αSMA and PDGFR-β in glioblastoma

To determine the amount of capillary-associated mural cells/pericytes, human glioma samples were stained for CD31 as a marker for endothelial cells and for αSMA and PDGFR-β as pericytic marker proteins. Both, αSMA and PDGFR-β showed a similarly heterogeneous distribution across glioma of all WHO grades rather correlating with the amount of capillaries or larger blood vessels in a distinct area (Figure 1A–J). However, there were no significant differences in the relative distribution of αSMA and PDGFR-β between low-grade glioma (LGG) and HGG (Figure 1K,L). To further investigate the possible impact of the observed heterogeneous vessel distribution related to malignant glioma progression, we analysed CD31 expression and examined vessel areas as well as the ratio of vessel count/vessel area. Even though the vessel density was not significantly altered between LGG and GBM (Figure 2A), and no significant correlation

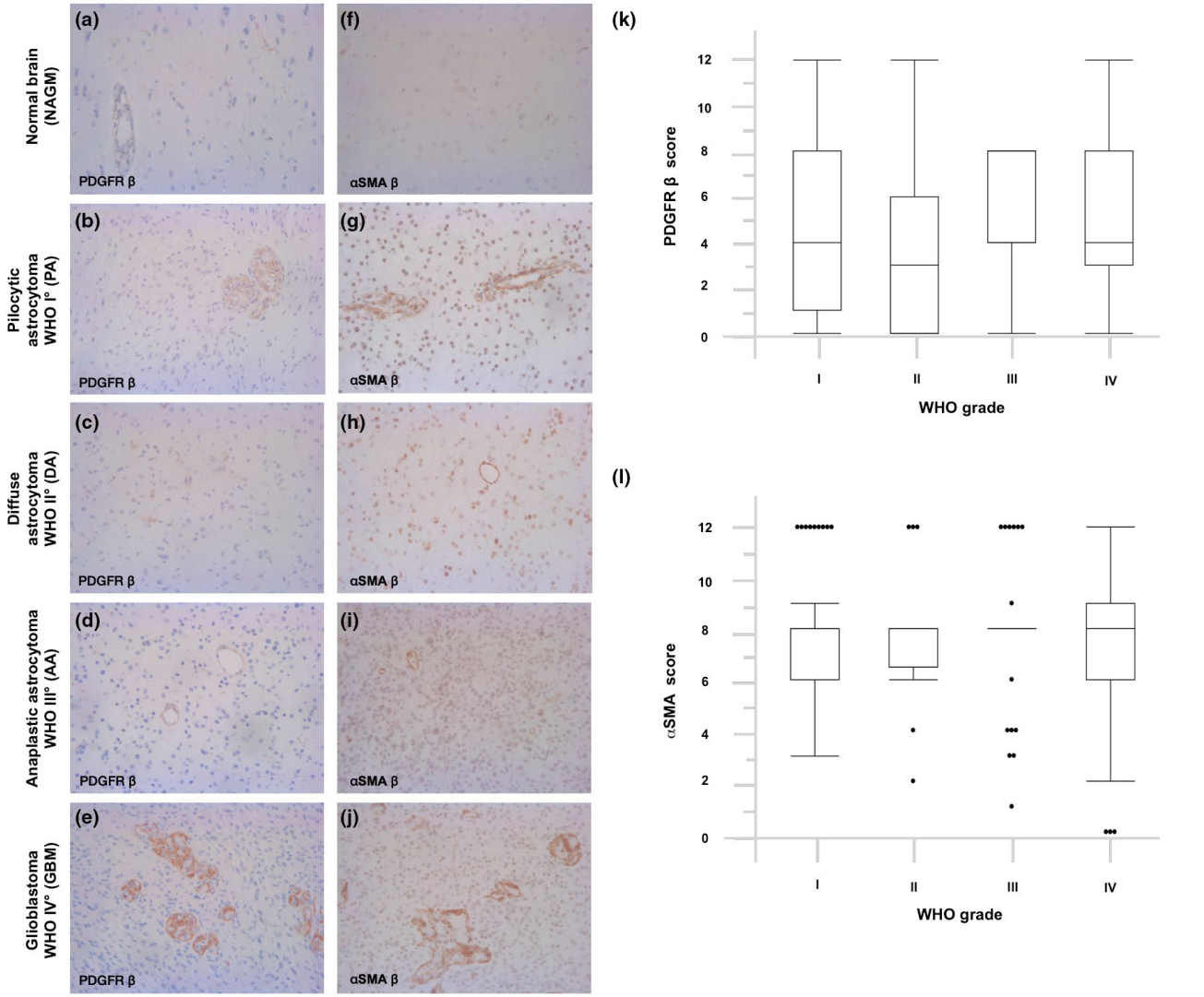

FIGURE 1 *αSMA and PDGFR-β expression in glioma of different WHO grades.* Immunohistochemistry of PDGFR-β (A–E) and αSMA (F–J) in normal brain tissue adjacent to glioma tissue (NAGM) and gliomas of WHO grades I–IV. Corresponding staining intensity scores (K, L) in gliomas of different WHO grades did not show significant statistical differences. Pilocytic astrocytomas (WHO grade I): $n = 47$; diffuse astrocytomas (WHO grade II): $n = 16$, anaplastic astrocytomas (WHO III): $n = 35$ and glioblastoma (WHO IV): $n = 253$

between high vessel density, αSMA or PDGFR-β expression and the survival of glioma patients (Figure 2B,C,E) was observed, the EMT transcription factor protein SLUG showed a significant correlation with the expression of both PDGFR-β and αSMA (Figure 2D,F; Figure S2). These findings indicate that tumour areas with a high amount of PDGFR-β- or αSMA-positive pericytes, also display significantly higher SLUG expression levels.

TGF-β induces SLUG and αSMA expression in pericytes

We then performed a gene expression analysis investigating the TCGA data set using the R2 platform to decipher potential factors being involved in the regulation of SLUG expression by activation of the SNAI2 gene. Transcriptional activation of SNAI2 strongly correlated with different collagen genes, αSMA ($R = 0.349$; $p = 3.1 \times 10^{-15}$), PDGFR-β ($R = 0.385$; $p = 1.3 \times 10^{-18}$) and very strongly with TGF-β1 ($R = 0.514$; $p = 9 \times 10^{-35}$, Table 1; for complete correlation analysis see Table S1). Since TGF-β is (a) a prominent pro-tumorigenic cytokine secreted by glioma cells, (b) involved in tumour-associated processes such as invasion, immunosuppression, inflammation and angiogenesis ([29], and for review see [30]), and (c) an important driver of EMT in epithelial tumours [15,16], we experimentally determined whether TGF-β modulates the expression of SLUG or αSMA in HBVP. We first examined whether the TGF-β pathway is functional in HBVP. For this, we incubated HBVP in the absence or presence of either TGF-β1 or -β2 and determined small worm phenotype Mothers Against Decapentaplegic (SMAD)-2 phosphorylation, a TGF-β signalling pathway downstream transducer protein. As shown in Figure 3A–C, treatment of HBVP with either TGF-β1 or -β2 induced SMAD-2 phosphorylation, an effect

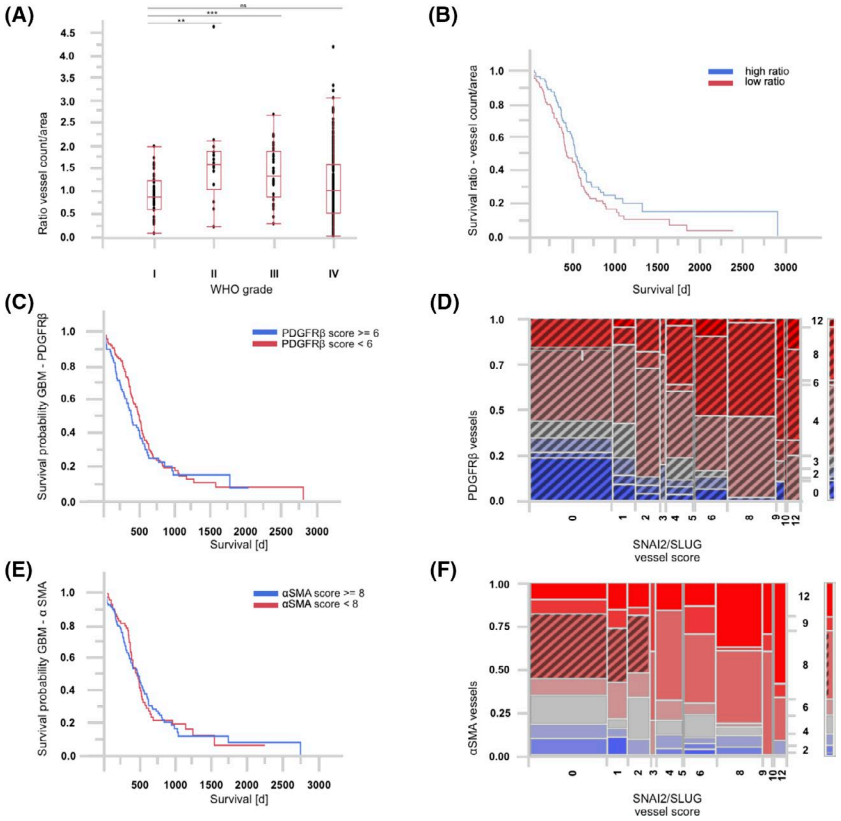

FIGURE 2 *Vessel density does not correlate with patient survival in GBM.* (A) Tissues were stained for CD31 and the ration of vessels counts/area was determined as described in the methods part. In GBM (WHO grade IV) survival analysis related to vessel density (B: median split for vessel count/area ratios; blue curve =high ratio; red curve =low ratio), related to PDGFR-β expression (C: blue curve =PDGFR-β expression level ≥6; red curve =PDGFR-β expression level <6) or related to αSMA expression (E: blue curve =αSMA expression level ≥8; red curve =αSMA expression level <8) did not show any significant differences. D/F. Correlation analyses for both (D) SNAI2/SLUG and PDGFR-β expression ($p = 0.0008$) as well as (F) SNAI2/SLUG and αSMA expression ($p = 0.0213$) revealed significant results as depicted in the contingency tables using the Pearson's chi-squared test. Pilocytic astrocytomas (WHO grade I): $n = 47$; diffuse astrocytomas (WHO grade II): $n = 16$ (WHO II), anaplastic astrocytomas (WHO III): $n = 35$ and glioblastoma (WHO IV): $n = 253$. (*$p < 0.05$; **$p < 0.01$; ***$p < 0.0001$)

that could be completely reverted by the addition of the TGF-β-neutralising antibody 1D11. In addition, we demonstrate that HBVP express the TGF-β receptor II (TGF-β-RII). Interestingly the expression of TGF-β-RII slightly increased by addition of TGF-β1, but not TGF-β2 (Figure 3D,E). These results illustrate that in HBVP the TGF-β signalling cascade is functionally intact.

We then determined whether TGF-β modulates the expression of SLUG or αSMA in HBVP. For this we cultured HBVP in the absence or presence of either TGF-β1 and/or TGF-β2 and determined SLUG and αSMA expression both on the mRNA and protein level. While basal expression of SLUG and αSMA was very low in untreated HBVP, both SLUG and αSMA mRNA was immediately upregulated as early as 1 h after treatment (Figure 3F, Figure S3). At protein level both proteins were upregulated 24 h after TGF-β1 and TGF-β2 treatment (Figure 3G–I). Of note, Slug levels increased considerably in HBVP upon stimulation at low TGF-β1 or -β2 concentrations of 0.1 and 1.0 ng/ml with no further relevant increase at higher concentrations (Figure 3G,H). This is most probably related to a saturation effect that is known to be dependent on cell type and cellular activation state.

TGF-β-mediated SLUG expression enhances pericytic cell clustering, proliferation and migration

We then tested whether an elevated SLUG expression also functionally modulates HBVP. For this, we first treated HBVP with TGF-β1 or TGF-β2, with conditioned medium from GBM cells (SN for supernatant), or upregulated SLUG by adenoviral infection using Ad-SLUG and determined the growth pattern of HBVP in these conditions. As shown in Figure 4, treatment with TGF-β, SN or enhanced expression of SLUG significantly altered the growth characteristics of HBVP cultures. Treated cultures showed a clustered growth, with cells possessing longer extensions, finally leading to a star-like network pattern. Induction of theses clustered growth morphology was detectable as early as 4 h after treatment (Figure S4). To determine whether the observed morphological changes were dependent on TGF-β, we also added the TGF-β antagonising antibody 1D11. Indeed, the addition of 1D11 reverted the morphological alterations of HBVP we observed by addition of either TGF-β or SN (Figure 4C, Figure S5). We then analysed whether TGF-β influences the capability of HBVP to proliferate and to migrate. Indeed, treatment of

TABLE 1 Summary of genes with a Pearson´s coefficient >0.5 correlating with SLUG/SNAI2 expression in glioma tissue

Gene		*R*	*p*-value	Function	Reference
PCOLCE	Procollagen C endopeptidase enhancer 1	0.615	1.20E−53	• enhances the activity of procollagen C-proteinases to participate in ECM re-construction • upregulated by TWST, promotes cancer cell migration and invasion	Moali et al., *JBC* 2005; 280: 24188 Wang et al., *Theranostics* 2019; 9(15): 4342
COL6A3	Collagen Type VI α3 chain	0.592	1.1E−48	• provides instructions for making one component of type VI collagen • promotes EMT via TGF-β in bladder cancer and influences angiogenesis	Huang et al., *Med Sci Monit*. 2018; 24: 5346
FBN1	Fibrillin 1	0.584	3.2E−47	• induced by TGF-β in metaplastic carcinoma undergoing EMT	Lien et al., *Pathology* 2019; 51(4): 375
COL1A1	Collagen type I α1 chain	0.582	8.5E−47	• promotes metastasis in colorectal cancer, tumor endothelial marker • contributes to angiogenesis and the development of deeply invasive mela-noma	Zhang et al., Mol Med Rep 2018; 17(4): 5037 Van Kempen et al., Int. J. Cancer 2008; 122: 1019
COL1A2	Collagen type I α2 chain	0.572	7.1E−45	• tumor endothelial marker • component of the brain tumor microenvironment	Liang et al. *J Neuro-Oncolog* 2008; 8:133
COL5A2	Collagen Type V α2 chain	0.565	1.3E−43	• in bladder cancer COL5A2 expression is linked to cell morphogenesis, angio-genesis and blood vessel development • highly enriched in GBM tissue	Meng et al., *Front Oncol*. 2019; 8: 659. Payne and Huang, *Mol Cancer Res*. 2013; 11(10): 1129
COL3A1	Collagen Type III α1 chain			• highly enriched in GBM tissue• directly correlated with glioma grade	Payne and Huang, *Mol Cancer Res*. 2013; 11(10): 1129 Gao et al., *Oncotarget* 2016; 7(43): 70494
LAMB1	Laminin Subunit β1	0.549	1.1E−40	• associated to glioma angiogenesis• enhanced translation of LAMB1 upon EMT in hepatocellular cancer	Chen et al., *Neuro Oncol*. 2014; 16(5): 637 Petz et al., Nucleic Acids Res. 2012; 40 (19): 9738
COL5A1	Collagen Type V α1 chain	0.542	2.0E−39	• COL5A1 expression associated with angiogenesis and the mesenchymal signature of TGF-β treated glioma cells	Mehta et al., *Cell Mol Life Sci*. 2018; 75: 385
LUM	Lumican	0.538	9.8E−39	• *Lumican* affects tumor cell functions, *tumor*–extracellular matrix interactions and *angiogenesis* • induces migration of bladder cancer cells	Nikitovic et al., *Matrix Biol*. 2014; 35: 206 Mao et al., *Translational Oncology* 2019; 12: 1072
RCN3	Reticulocalbin 3	0.532	1.0E−37	• negatively regulates the secretion of type I and type III collagens	Martinez et al., *Sci Rep*. 2017; 22;7(1): 12192.
FSTL1	Follistatin Like 1	0.526	9.9E−37	• angiogenic factor, suppresses tumor cell proliferation, invasion and survival in NSCLC	Ni et al., *Oncol Rep* 2018; 39(1): 13
SERPINH1	Serpin H 1/heat shock protein 47/ Colligin 2	0.52	7.0E−36	• promotes GBM stemlike cell survival by modulating the tumor microenviron-ment through TGF-β • expressed especially in the glioma neovasculature	Jiang et al., *ACS Chem Neurosci*. 2017; 8(1): 128 Mustafa et al., *Gene Regul Syst Bio*. 2010; 4: 103

(Continues)

TABLE 1 (Continued)

Gene		*R*	*p*-value	Function	Reference
TGFB1	Transforming growth factor β1	0.514	9.0E−35	• potent multifunctional cytokine in glioma, involved in cell migration and invasion, immuno-suppression, angiogenesis and inflammation	Massague, *Nat Rev Mol Cell Biol* 2012; 13(10): 616 Pickup et al., *Nat Rev Cancer* 2013; 13(11): 788
ADAM12	Disintegrin and metallo-proteinase domain-containing protein 12/ Meltrin	0.501	8.9E−33	• ADAM12 expression in breast tumor cells correlated with upregulation of proangiogenic and downregulation of antiangiogenic factors • Protease of matrix and adhesion proteins, upregulated in GBM	Roy et al., *Mol Cancer Res*. 2017; 15(11): 1608 Bougnaud et al., *Oncotarget*. 2016; 7(22): 31955

HBVP with either TGF-β1, -β2, both, or with conditioned medium from LN-229 glioma cells significantly induced proliferation and migration (Figure 5A/B). Since migration is often coupled to an elevated metabolic activity (for review see [31]), we also measured the mitochondrial activity of TGF-β-treated HBVP and found that the elevated migration capability is paralleled by a higher metabolic activity (Figure 5C). To determine whether these observed effects are associated with the elevated SLUG expression, we observed in HBVP upon cultivation in the presence of TGF-β, we knocked down SLUG by siRNA transfection prior to treatment (Figure S6). Knockdown of SLUG completely inhibited the capability of TGF-β or SN to induce proliferation, migration and metabolic activity in HBVP (Figure 5). In addition, we neutralised TGF-β by the addition of TGF-β antagonising antibody 1D11. While 1D11 significantly mitigated the TGF-β-mediated induction of proliferation of HBVP, there was only a trend in the reduction of the metabolic activity and cell migration (Figure 6).

DISCUSSION

In GBM, the presence of vascular proliferation is a diagnostic hallmark separating them from lower grade diffuse gliomas, the latter exhibiting a significantly better prognosis.[32] This suggests that probably not the amount of tumour-associated vessels, but especially an altered vascular morphology is associated with brain tumour malignancy.[33] In a previous study, we have shown that the key EMT transcription factor SLUG is exclusively expressed in pericytes of vascular proliferates in the group of highly angiogenic GBM (WHO IV), while being absent in less angiogenic diffuse gliomas (astrocytoma WHO II and III), in pericytes covering tumour remote vessels in GBM as well as in glioma cells of all WHO grades.[12] Pericytes play an essential role in maintaining vessels and therefore also BBB integrity. Degenerative blood vessels are observed in diseases like hereditary cerebral haemorrhage [34] while vascular proliferation and abnormalities are common in GBM.[33] The finding that glioma vessel-associated pericytes (GA-Peris) strongly express EMT transcription factors in vascular proliferation [12] along with a pronounced morphological alteration of GBM-associated vessels suggests that these non-neoplastic cells undergo an EMT-related activation process during glioma-associated neoangiogenic processes.

In a cohort of glioma patients (WHO I–IV), we determined vessel density by CD31 staining as well as pericyte density by staining for αSMA and PDGFR-β. Interestingly and partly unexpected, both vessel density as well as the amount of αSMA and PDGFR-β positive pericytes in the tumour area, were not significantly different in LGG as compared to GBM and did also not correlate with patient survival (Figures 1 and 2). However, the expression of SLUG strongly correlated with that of the pericytic lineage markers αSMA and PDGFR-β, indicating that, in GBM, pericytes are mainly SLUG positive (Figure 2D,F). Nevertheless, these data do not clarify how SLUG expression is induced in GA-Peris. It has been debated whether these SLUG-positive pericytes originate from human mesenchymal

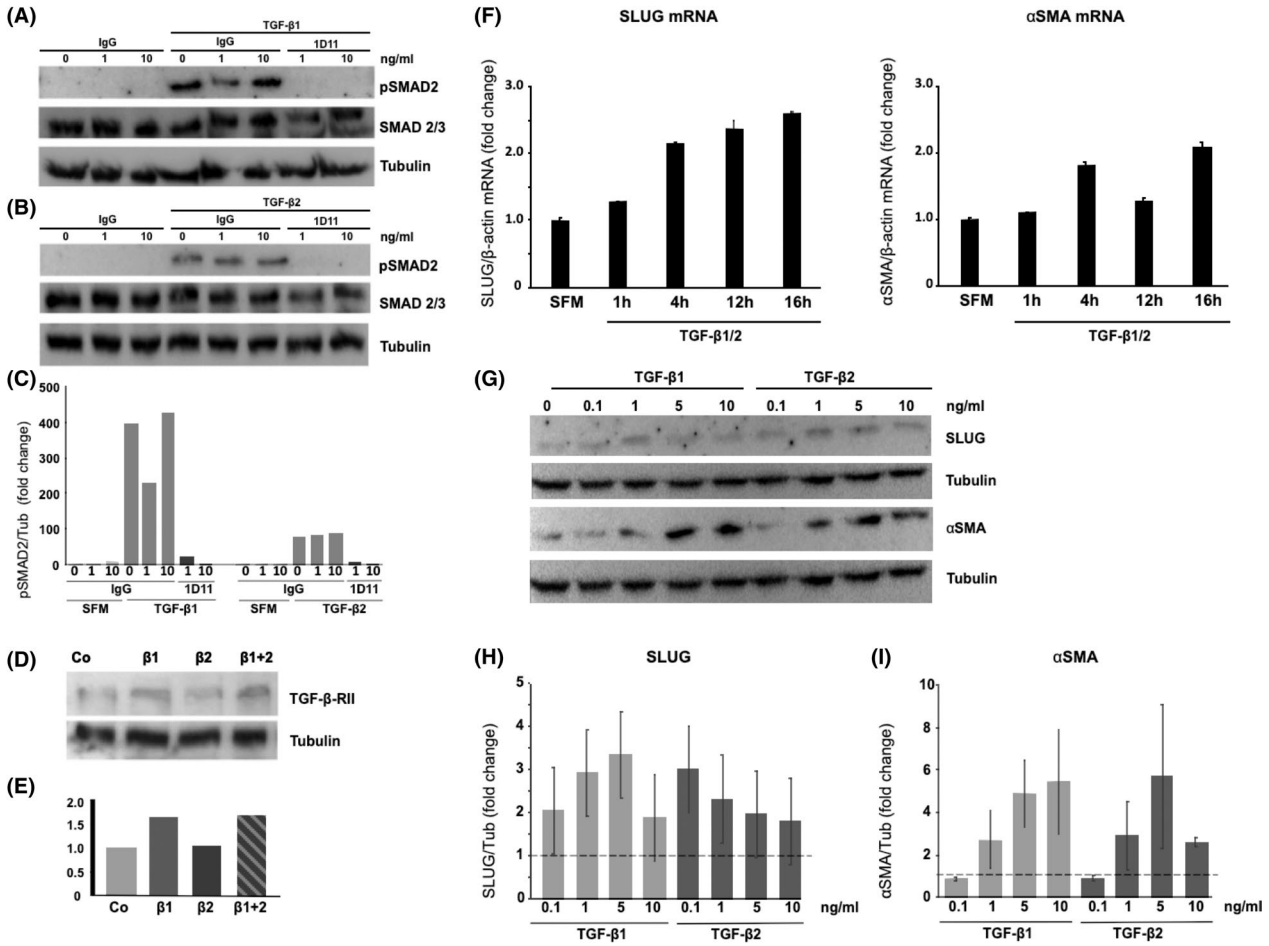

FIGURE 3 *In HBVP TGF-β induces SLUG and αSMA expression.* (A–E) The TGF-β signal pathway is functional in HBVP. A/B/C. HBVPs were incubated for 30 min in the presence of or absence of 10 ng/ml TGF-β1 (A) or -β2 (B) in combination with IgG as an isotype control or with the TGF-β-neutralising antibody 1D11. Lysates were prepared and phospho-SMAD2 as well as tubulin as a housekeeping gene were determined by immunoblot. (C) Quantification of pSMAD upon TGF-β treatment as indicated in A and B. Tubulin was used for normalisation of protein expression. (D) HBVPs were incubated in the absence or presence of 10 ng/ml TGF-β1, TGF-β2 or both. Lysates were prepared and TGF-β-RII expression was determined by immunoblot. Tubulin serves as control. (E) Quantification of TGF-β-RII as described in (D), Tubulin expression was used for normalisation. (F) HBVPs were incubated in the presence or absence of combined TGF-β1 and -β2 (each 10 ng/ml) for increasing time periods. Gene expression was determined by q-PCR (one representative experiment is shown). (G) HBVPs were cultivated for 24 h in the presence of increasing concentrations of TGF-β1 and/or TGF-β2. Protein expression of SLUG and αSMA was determined by immunoblot. H/I: Quantification of SLUG (H) and αSMA protein (I) in TGF-β-treated HBVP as indicated in G. Tubulin expression served for normalisation (n = 2, SD)

stem cells (hMSC) or from pericytic progenitors that are recruited from outside the tumour or even from outside the brain during neovascularisation. However, this seems to be unlikely since the large number of hMSC or pericytic progenitors would have to pass the endothelial cell layer of glioma vessels, although experimental data indicated that after intravenous injection, MSCs are able to graft into the tumour vasculature.[35] Since it has been previously shown that glioma cells are able to modulate the function of pericytes by shifting them towards an immunosuppressive cell type,[19] it might be more reasonable that SLUG expression in GA-Peris might be induced by cytokines released form adjacent tumour cells. TGF-β, a multifunctional cytokine highly secreted by HGG,[17] is an important driver of EMT.[36] Based on these data and our TCGA-correlation analysis, we examined the effects of TGF-β on pericytes. Indeed, paralleled by the upregulation of SLUG, treatment of HBVP with TGF-β or conditioned medium from glioma cells led to an activation of HBVP, indicated by cellular clustering, enhanced proliferation as well as by the induction of cell migration (Figures 3–5, Figures S4 and S5). Importantly, the TGF-β responsive downstream gene SNAI2, coding for the EMT transcriptional regulator SLUG, seems to be at least partially responsible for these effects. On the one hand, knockdown of SLUG in HBVP abolished both TGF-β- and SN-mediated enhanced proliferation and cell migration (Figure 5), and on the other hand, exogenous SLUG overexpression in HBVPs induced the same morphological changes as TGF-β or G-SN. Under the latter conditions, HBVPs grow in a clustered, star-like pattern (Figure 4). This clustered growth is comparable to that demonstrated by Nakagomi *et al.* for ischaemic mouse brain vascular pericytes (iPC).[37] Interestingly,

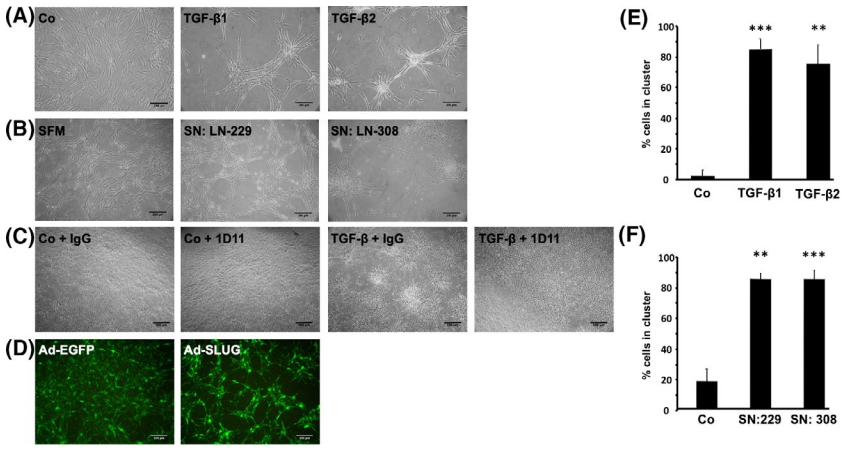

FIGURE 4 *Morphology of HBVP changed by addition of TGF-β,by cultivation in glioma cell supernatants or by overexpressing SLUG*. A/B. HBVPs were cultivated in TGF-β1 or -β2 (10 ng/ml each) containing medium (A) or in medium that was harvested from glioma cells (B, SFM: serum-free medium serving as control). (C) HBVPs were cultured in the presence of TGF-β1 and -β2 (1 ng/ml each) in combination with TGF-β-antagonising antibody 1D11 in a 100-fold excess or IgG as an isotype control antibody. One representative experiment is shown. (D) HBVPs were infected with either Ad-EGFP as control or with Ad-SLUG (30 MOI). After 24 h of cultivation microscopic photographs were taken. One representative photograph is shown (A, B: $n = 6$; C: $n = 3$, D: $n = 2$). E/F. Quantification of star-like clusters after treatment with TGF-β (E) or after cultivation in medium harvested from glioma cells (F) ($n = 3$; $^{*}p < 0.05$; $^{**}p < 0.01$; $^{***}p < 0.001$, SD)

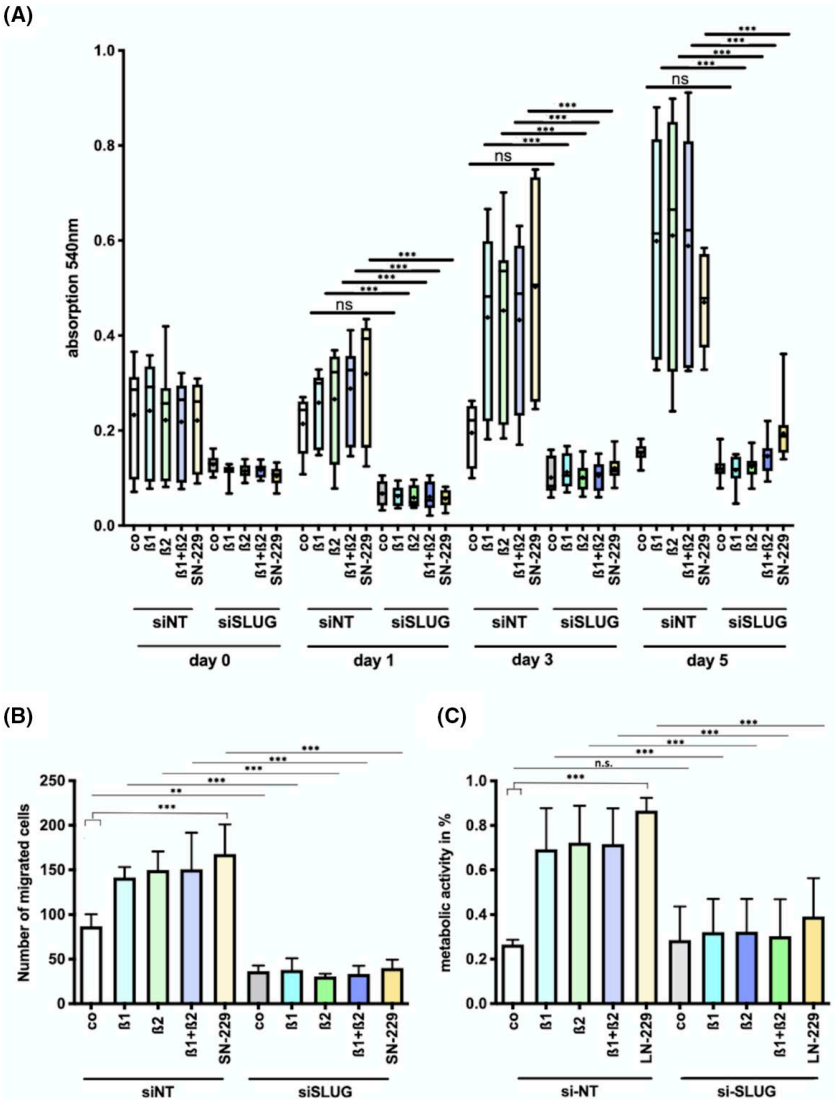

FIGURE 5 *Knockdown of SLUG functionally modulates HBVP*. HBVPs were transfected with SLUG-specific or non-target siRNA and were treated with either serum-deprived medium (SF), TGF-β1 or -β2 or both (each 10 ng/ml) or conditioned medium from LN-229 glioma cells (SN-229). (A) Cell density was assessed by crystal violet staining every second day ($n = 3$, SD). (B) Cell mobility was analysed by transwell Boyden chamber assays as described in the material and methods part ($n = 3$, SD). (C) Mitochondrial activity was determined 72 h after transfection using the MTT assay ($n = 3$, SD). Proliferation, migration and metabolic activity changes were statistically analysed using ANOVA followed by Tukey's test (n.s.: not significant; $^{*}p < 0.05$, $^{**}p < 0.01$; $^{***}p < 0.001$)

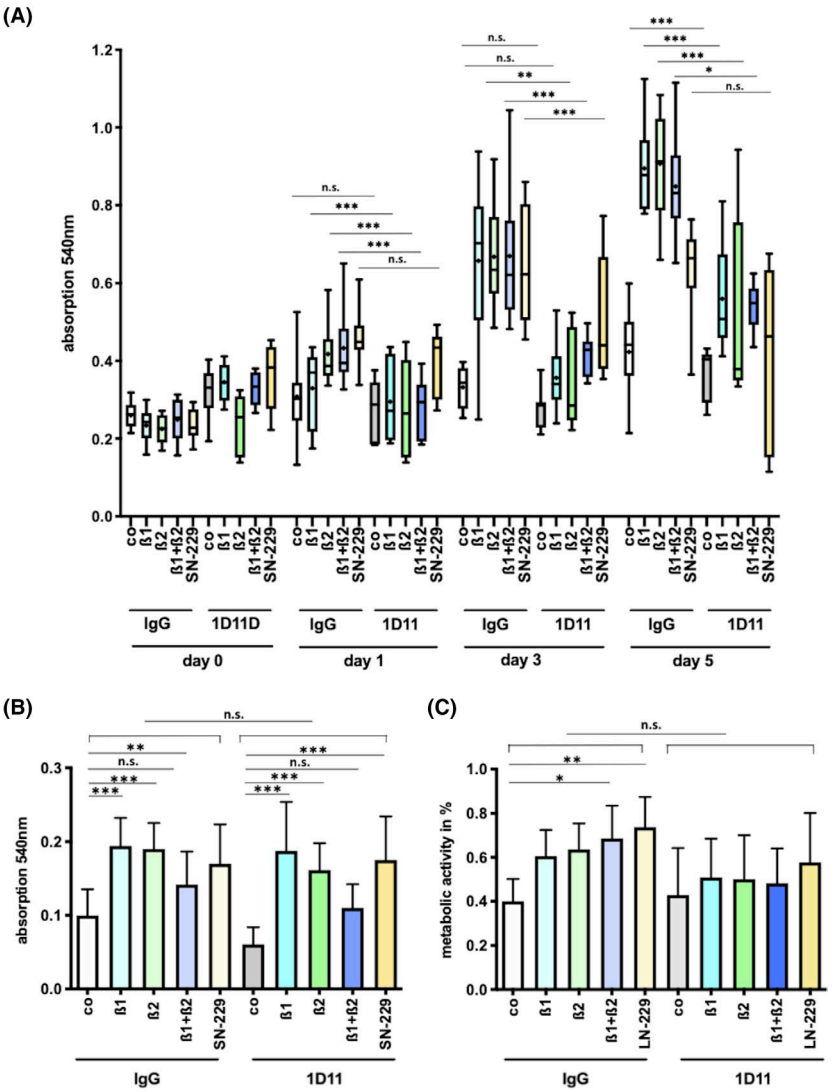

FIGURE 6 *Neutralisation of TGF-β activity reduces TGF-β- and SN-mediated induction of HBVP proliferation,but not migration and metabolic activity.* HBVPs were cultivated in the absence or presence of TGF-β1, -β2, TGF-β1+2 or SN from LN-229 glioma cells (SN-229) in combination with the TGF-β-antagonising antibody 1D11 in a 100-fold excess, or IgG as an isotype control antibody. (A) Cell density was assessed by crystal violet staining every second day (n = 3, SD). (B) Cell mobility was analysed by transwell Boyden chamber assays as described (n = 5, SD). (C) Mitochondrial activity was determined using the WST1 assay (n = 3, SD). Proliferation, migration and metabolic activity changes were analysed using ANOVA followed by Tukey's test (n.s.: not significant; $^{*}p < 0.05$, $^{**}p < 0.01$; $^{***}p < 0.001$)

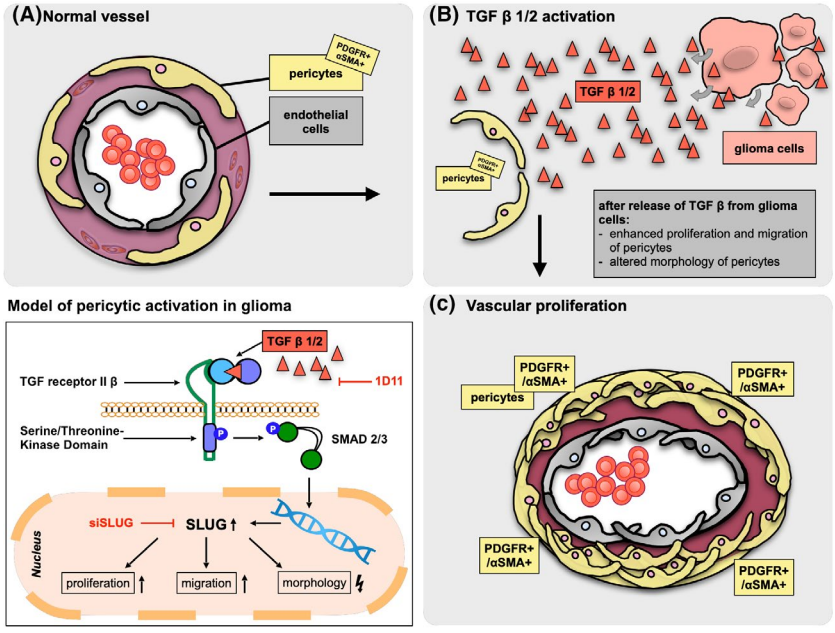

FIGURE 7 *Model of pericytic activation in glioma*. (A) Scheme of a normal brain vessel. B/C. TGF-β released by GBM cells (B) modulates the function of tumour adjacent pericytes leading, via upregulation of EMT factors like SLUG, to (C) proliferation, migration and morphological changes of PDGFR-β^{+}/ αSMA^{+} pericytes

like GA-Peris, iPCs also express PDGFR-β and SLUG. In this regard, the observed changes in the cells growth characteristics seemed to be induced by TGF-β since addition of the TGF-β-neutralising antibody 1D11 abolished this effect (Figure 4C, Figure S5).

It has been recently shown in a mouse model of ischaemic retinopathy that during pathological neovascularisation abnormal, αSMA-expressing pericytes cover the angiogenic sprouts and pathological neovascular tufts. Disturbance of the homeostasis of pericyte migration in this model results in vascular abnormality, vessel leakiness and pathology.[38] In HBVP treated with TGF-β or SN, their capacity to proliferate was significantly enhanced, an effect that was reverted by knocking down SLUG or by neutralising TGF-β activity (Figures 5, 6). Additionally, both cell migration and metabolic mitochondrial activity, the latter coupled to cell motility in many cancer cells (for review see [31]), was also induced by TGF-β or by the cultivation of HBVP in SN. This effect was completely abolished if the induction of SLUG in HBVP was prohibited by transfection with SLUG siRNA prior to treatment (Figure 5), indicating that also in HBVP EMT proteins like SLUG are important inducers of cell motility. However, while the knockdown of SLUG completely prevented the TGF-β-mediated induction of mitochondrial activity and migration in HBVP, this was not the case if TGF-β activity was neutralised by addition of 1D11. This suggests that a generally and nearly complete reduction of SLUG that was achieved by siRNA was functionally more potent than an upstream inhibition of TGF-β that leaves a basal amount of SLUG protein in the cells (Figures 5, 6, Figure S6).

The elevated migration of SLUG-expressing HBVP as well as their elevated proliferative properties might explain why newly formed vessels often show a chaotic structure in GBM and why in these newly built, tumour-associated vessels the BBB is often disrupted. The increased proliferation capacity of GA-Peris induced by a hypoxic tumour microenvironment might also explain the presence of vascular proliferation in GBM. In these proliferations, many cells are PDGFR-β, αSMA and SLUG positive[12] indicating that not endothelial cells, but pericytes are major participants in these structures. However, whether the TGF-β and SLUG-mediated effects we observed in vitro in HBVP can be easily transferred to the in vivo situation needs further investigations and the generation of a mouse glioma model that allows for SLUG knockdown selectively in tumour-adjacent pericytes.

CONCLUSIONS

In GA-Peris, the observed elevated SLUG expression, paralleled by the induction of cell proliferation, mitochondrial activity and cell migration, is induced by TGF-β, a cytokine highly expressed by glioma cells. SLUG expression in pericytes is important for both proliferation as well as migration of pericytes at least in cell culture, since neutralisation of TGF-β or knocking down SLUG mitigated or even abolished proliferation, cell motility, metabolic activity and morphological alterations in HBVP (see Figure 7 as a summary model). Our data indicate that GBM cells actively modulate neovascularisation not only by modulating endothelial cells, but also by influencing the function and characteristics of adjacent vessel-associated pericytes. This process might be responsible for the formation of an unstructured tumour vasculature as well as for the breakdown of the BBB in the tumour area.

ETHICS APPROVAL

For patient's material, a written informed consent was obtained from all patients. The use of patient material was approved by the local ethics committee (GS-04/09 and GS-249/11). The manuscript does not contain any individual person's data in any form.

ACKNOWLEDGEMENTS

Michel Mittelbronn would like to thank the Luxembourg National Research Fond (FNR) for the support (FNR PEARL P16/BM/11192868 grant).

CONFLICT OF INTEREST

The authors declare that they have no competing interests.

AUTHOR CONTRIBUTIONS

MM and UN designed and supervised the study. MM, UN and NMW wrote the manuscript. NMW, JE, LM, EII, AEB, AG, FF, PB, UN and KD performed experiments and analysed data. MM and PNH characterised the human tissues samples. MM, UN and PNH discussed data.

PEER REVIEW

The peer review history for this article is available at https://publons.com/publon/10.1111/nan.12714.

DATA AVAILABILITY STATEMENT

The data sets generated during and/or analysed during the current study are available from the corresponding author on reasonable request.

ORCID

Patrick N. Harter https://orcid.org/0000-0001-5530-6910
Ulrike Naumann https://orcid.org/0000-0003-3555-5703

REFERENCES

1. Woehrer A, Bauchet L, Barnholtz-Sloan JS. Glioblastoma survival: has it improved? Evidence from population-based studies. *Curr Opin Neurol*. 2014;27:666-674.
2. Hardee ME, Zagzag D. Mechanisms of glioma-associated neovascularization. *Am J Pathol*. 2012;181:1126-1141.
3. Joseph JV, Balasubramaniyan V, Walenkamp A, Kruyt FA. TGF-beta as a therapeutic target in high grade gliomas - promises and challenges. *Biochem Pharmacol*. 2013;85:478-485.
4. Oliver L, Olivier C, Marhuenda FB, Campone M, Vallette FM. Hypoxia and the malignant glioma microenvironment: regulation and implications for therapy. *Curr Mol Pharmacol*. 2009;2:263-284.
5. Jordan NV, Johnson GL, Abell AN. Tracking the intermediate stages of epithelial-mesenchymal transition in epithelial stem cells and cancer. *Cell Cycle*. 2011;10:2865-2873.

6. Makker A, Goel MM. Tumor progression, metastasis, and modulators of epithelial-mesenchymal transition in endometrioid endometrial carcinoma: an update. *Endocr Relat Cancer*. 2016;23:R85-R111.
7. Davidson B, Trope CG, Reich R. Epithelial-mesenchymal transition in ovarian carcinoma. *Front Oncol*. 2012;2:33.
8. Matejka VM, Finek J, Kralickova M. Epithelial-mesenchymal transition in tumor tissue and its role for metastatic spread of cancer. *Klinicka Onkologie*. 2017;30(1):20-27.
9. Hamidi S, Sheng G. Epithelial-mesenchymal transition in haematopoietic stem cell development and homeostasis. *J Biochem*. 2018;164:265-275.
10. Jolly MK, Ward C, Eapen MS, et al. Epithelial-mesenchymal transition, a spectrum of states: role in lung development, homeostasis, and disease. *Dev Dyn*. 2018;247:346-358.
11. Phillips HS, Kharbanda S, Chen R, et al. Molecular subclasses of high-grade glioma predict prognosis, delineate a pattern of disease progression, and resemble stages in neurogenesis. *Cancer Cell*. 2006;9:157-173.
12. Mäder L, Blank AE, Capper D, et al. Pericytes/vessel-associated mural cells (VAMCs) are the major source of key epithelial-mesenchymal transition (EMT) factors SLUG and TWIST in human glioma. *Oncotarget*. 2018;9:24041-24053.
13. Seifert M, Garbe M, Friedrich B, Mittelbronn M, Klink B. Comparative transcriptomics reveals similarities and differences between astrocytoma grades. *BMC Cancer*. 2015;15:952.
14. Liu Y, Hu H, Wang K, et al. Multidimensional analysis of gene expression reveals TGFB1I1-induced EMT contributes to malignant progression of astrocytomas. *Oncotarget*. 2014;5:12593-12606.
15. Moustakas A, Heldin P. TGFbeta and matrix-regulated epithelial to mesenchymal transition. *Biochim Biophys Acta*. 2014;1840:2621-2634.
16. Miyazono K, Ehata S, Koinuma D. Tumor-promoting functions of transforming growth factor-beta in progression of cancer. *Ups J Med Sci*. 2012;117:143-152.
17. Roy LO, Poirier MB, Fortin D. Transforming growth factor-beta and its implication in the malignancy of gliomas. *Target Oncol*. 2015;10:1-14.
18. Liebner S, Dijkhuizen RM, Reiss Y, Plate KH, Agalliu D, Constantin G. Functional morphology of the blood-brain barrier in health and disease. *Acta Neuropathol*. 2018;135:311-336.
19. Ochs K, Sahm F, Opitz CA, et al. Immature mesenchymal stem cell-like pericytes as mediators of immunosuppression in human malignant glioma. *J Neuroimmunol*. 2013;265:106-116.
20. Caspani EM, Crossley PH, Redondo-Garcia C, Martinez S. Glioblastoma: a pathogenic crosstalk between tumor cells and pericytes. *PLoS One*. 2014;9:e101402.
21. Ishii N, Maier D, Merlo A, et al. Frequent co-alterations of TP53, p16/CDKN2A, p14ARF, PTEN tumor suppressor genes in human glioma cell lines. *Brain Pathol*. 1999;9:469-479.
22. Armento A, Ilina EI, Kaoma T, et al. Carboxypeptidase E transmits its anti-migratory function in glioma cells via transcriptional regulation of cell architecture and motility regulating factors. *Int J Oncol*. 2017;51(2):702–714.
23. Naumann U, Kügler S, Wolburg H, et al. Chimeric tumor suppressor 1, a p53-derived chimeric tumor suppressor gene, kills p53 mutant and p53 wild-type glioma cells in synergy with irradiation and CD95 ligand. *Cancer Res*. 2001;61:5833-5842.
24. Ruifrok AC, Johnston DA. Quantification of histochemical staining by color deconvolution. *Anal Quant Cytol Histol*. 2001;23:291-299.
25. Brink AD, Pendoch NE. Minimum cross-entropy threshold selection. *Pattern Recogn*. 1996;29:179-188.
26. Bartussek C, Naumann U, Weller M. Accumulation of mutant p53 (V143A) modulates the growth, clonogenicity, and radiochemosensitivity of malignant glioma cells independent of endogenous p53 status. *Exp Cell Res*. 1999;253:432-439.
27. Mantwill K, Naumann U, Seznec J, et al. YB-1 dependent oncolytic adenovirus efficiently inhibits tumor growth of glioma cancer stem like cells. *J Transl Med*. 2013;11:216.
28. Schötterl S, Hubner M, Armento A, et al. Viscumins functionally modulate cell motility-associated gene expression. *Int J Oncol*. 2017;50:684-696.
29. Dieterich LC, Mellberg S, Langenkamp E, et al. Transcriptional profiling of human glioblastoma vessels indicates a key role of VEGF-A and TGFbeta2 in vascular abnormalization. *J Pathol*. 2012;228:378-390.
30. Kaminska B, Kocyk M, Kijewska M. TGF beta signaling and its role in glioma pathogenesis. *Adv Exp Med Biol*. 2013;986:171-187.
31. Colquhoun A. Cell biology-metabolic crosstalk in glioma. *Int J Biochem Cell Biol*. 2017;89:171-181.
32. Louis DN, Ohgaki H, Wiestler OD, et al. The 2007 WHO classification of tumours of the central nervous system. *Acta Neuropathol*. 2007;114:97-109.
33. Birner P, Piribauer M, Fischer I, et al. Vascular patterns in glioblastoma influence clinical outcome and associate with variable expression of angiogenic proteins: evidence for distinct angiogenic subtypes. *Brain Pathol*. 2003;13:133-143.
34. Verbeek MM, de Waal RM, Schipper JJ, Van Nostrand WE. Rapid degeneration of cultured human brain pericytes by amyloid beta protein. *J Neurochem*. 1997;68:1135-1141.
35. Bexell D, Gunnarsson S, Tormin A, et al. Bone marrow multipotent mesenchymal stroma cells act as pericyte-like migratory vehicles in experimental gliomas. *Mol Ther*. 2009;17:183-190.
36. Kahata K, Dadras MS, Moustakas A. TGF-beta family signaling in epithelial differentiation and epithelial-mesenchymal transition. *Cold Spring Harb Perspect Biol*. 2018;10(3):a031997.
37. Nakagomi T, Kubo S, Nakano-Doi A, et al. Brain vascular pericytes following ischemia have multipotential stem cell activity to differentiate into neural and vascular lineage cells. *Stem Cells*. 2015;33:1962–1974.
38. Dubrac A, Kunzel SE, Kunzel SH, et al. NCK-dependent pericyte migration promotes pathological neovascularization in ischemic retinopathy. *Nat Commun*. 2018;9:3463.

SUPPORTING INFORMATION

Additional supporting information may be found online in the Supporting Information section.

How to cite this article: Wirsik NM, Ehlers J, Mäder L, et al. TGF-β activates pericytes via induction of the epithelial-to-mesenchymal transition protein SLUG in glioblastoma. *Neuropathol Appl Neurobiol*. 2021;00:1–13. https://doi.org/10.1111/nan.12714